

# Optimisation of Dynamic Gait for Small Bipedal Robots

Peter Gibbons, Martin Mason, Alexandre Vicente, Guido Bugmann and Phil Culverhouse

Centre for Robotics and Neural Systems, School of Computing & Mathematics, University of Plymouth  
Plymouth, PL4 8AA, UK

peter.gibbons@plymouth.ac.uk

martin.mason@postgrad.plymouth.ac.uk

guido.bugmann@plymouth.ac.uk

phil.culverhouse@plymouth.ac.uk.

**Abstract**— This paper describes a compact gait generator that runs on the on-board ATmega128 microcontroller of the Robotis Bioloid robot platform. An overview of the parameters that effect dynamic gait is included along with a discussion of how these are implemented in a servo skeleton. The gait parameters are stride height, hip swing amplitude and step period. The paper reports on the optimisation of these parameters through a systematic exploration of the parameter space. The quality of the parameters is evaluated in terms of lateral head movement and foot clearance. This research was facilitated by the use of an online wireless programming interface that enables rapid testing of all the gait parameters. The gait quality was observed to be optimal at shorter step periods and larger stride heights.

## I. INTRODUCTION

To be competitive in robot football the biped must travel quickly between one location and another. One strategy to achieve this is to have a robust dynamic gait that is stable under small perturbing external forces. This has been investigated previously in [1, 2]. The gait under investigation has no sensor feedback and thus must be highly stable to deal with the wide variety of environmental conditions, such as an uneven floor or different surface textures that will be encountered. To achieve a stable gait in the absence of sensor feedback, it is important to understand the underlying parameters that effect biped motion and to optimise these parameters to suit the environment. In this paper we introduce a model of gait parameters, discuss measures of gait stability and present preliminary results for a stable dynamic gait based on the characterisation of three important dynamic properties.

A bipedal humanoid platform designed at the University of Plymouth by Wolf et al. [3, 4] and based on the Bioloid servo skeleton by Robotis (Fig. 1) is used as a test bed to develop a set of parameters to optimise a dynamic gait for the FIRA 2009 RoboWorld Cup competition.

## II. OVERVIEW OF DYNAMIC GAIT

A dynamically stable gait is one that has a repetitive motion that remains unchanged over a given time of observation or task. This means that the oscillating motion of the legs has to be inherently stable and resistant to small surface defects and changes in surface. In order to create a stable gait we first would like to be able to position the robot's foot precisely in space.



Fig. 1 University of Plymouth Biped.

### A. Inverse Kinematics for Positioning

An inverse kinematic model of the legs of the robot is created by modelling the robots legs as a two link system. The accessible plane of operation for each leg is segmented into a 70x150 grid and the joint angles are pre-computed for each of these points and saved as a lookup table (Fig. 2).

The lookup table is sized to occupy 2x32K and is stored in the embedded processor of the robot. When desired X (horizontal) and Y (vertical) coordinates are calculated from the gait driving function, the joint angles are retrieved from the lookup table and applied to the planar

hip, knee and foot servo positions. If the hip rotates then the kinematic plane is also rotated and the lookup table is used to determine the servo positions.

### B. Gait Generation

To establish the dynamic gait, a sinusoid was mapped to the X and Y coordinates of each foot with the parameters of stride amplitude and period. The coordinates of the first foot are calculated by the following function:

$$X = \text{Stride\_Length} * \cos\left(\frac{2\pi t}{T}\right) + X\_Offset \quad (1)$$

$$Y = \text{Stride\_Height} * \sin\left(\frac{2\pi t}{T}\right) + Y\_Offset \quad (2)$$

These two functions create an ellipsoid with a horizontal axis of two times the stride length and a vertical axis of two times the stride height. The second foot is mapped out of phase by  $\pi$  radians from the first foot. Once the joint angles are calculated, the servo velocities are calculated by determining the rotation angle of each servo and then ensuring that all servos take the same time to complete the movement. This basic sinusoidal function serves as the building block for the dynamic gait, but a number of other dynamic and static parameters are also implemented.

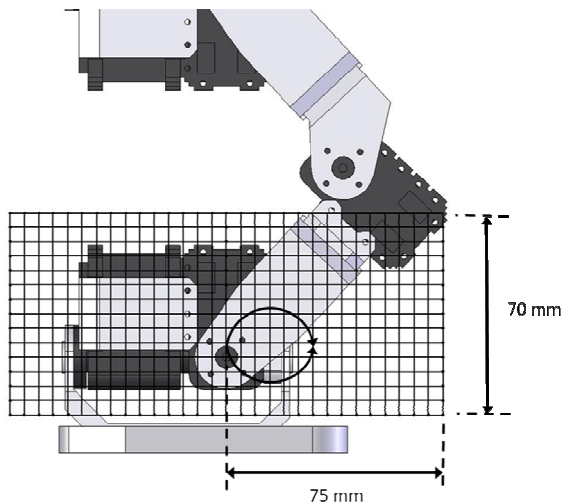


Fig. 2 The joint angles for each of the grid points are pre-computed and stored in the onboard microprocessor. The curve indicates the trajectory of the foot defined by (1) & (2).

### C. Static Parameters

The following properties are static in that they remain as constants that affect the posture of the robot.

1) *Tilt*: To maintain a stable dynamic walk, the robot's centre of mass should be positioned slightly forward (Fig. 3). Depending on the geometry of the robot and its current mass configuration, the robot should be inclined

forward by adding some additional rotation to the planar hip servos.

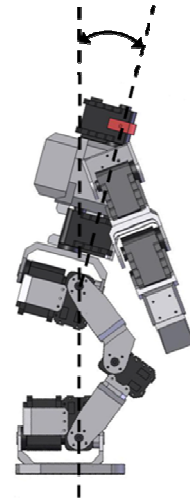


Fig. 3 The tilt inclines the centre of gravity to balance the robot.

2) *Body Offset*: This defines how erect the robot stands (Fig. 4). When the Y component of the foot's position is calculated, a constant offset is added to change the overall height of the stance. Since the origin is defined as the foot coordinates with the legs fully straight, without a body offset, the calculated Y positions (equation 2) will become negative and thus out of bounds for the inverse kinematic model.

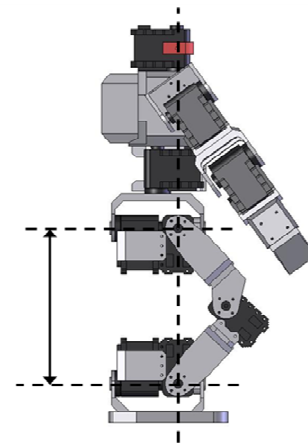


Fig. 4 The body offset shifts the vertical origin of the coordinate system through which the foot moves.

3) *Camber*: This adds an offset to the rotational hip servo and a mirroring offset to the rotational foot servo (Fig. 5). With a camber of zero, the robot stands with its legs aligned parallel. As a negative camber is added, the legs spread outward providing a force pointing inward which helps to increase stability.

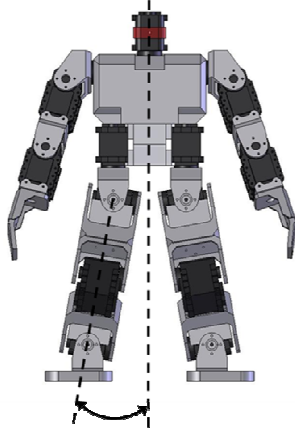


Fig. 5 Camber introduces a rotational offset on the hip and ankle joints to increase lateral stability and prevent collisions between servo skeleton elements.

#### D. Dynamic Parameters

These parameters change as a function of time during the motion of the robot. The overall motion of the legs was discussed previously as a sinusoidal function mapped to the plane defined by the vector from the hip to the knee and the vector from the knee to the ankle.

1) *Swing*: In order for the robot to move, it has to shift its centre of mass from one foot to the other (Fig. 6). In this simple implementation, a linear function is mapped to the rotational hip servos with the same period as the sinusoid (Fig. 7) and a mirrored function is mapped to the rotational foot servos. This causes the robot to sway back and forth continually shifting its centre of mass from one foot to the other. The current implementation is not ideal and is a remnant from decisions made during competition. We would like to have the hip swing occur ahead of the foot clearance to increase the mass over the foot that is to remain planted.

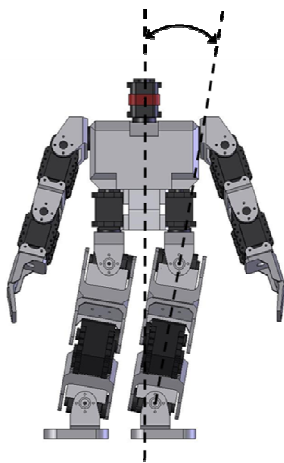


Fig. 6 Swing Amplitude controls how far the centre of mass of the robot shifts.

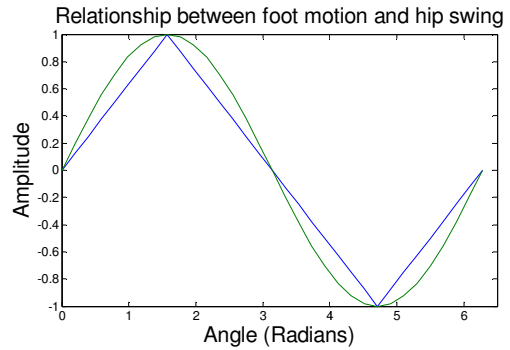


Fig. 7 The relationship between the swing of the hips (straight line) and the motion of the feet (curved line).

The following figures summarise the parameters that determine the gait and how they are used to calculate the servo positions.

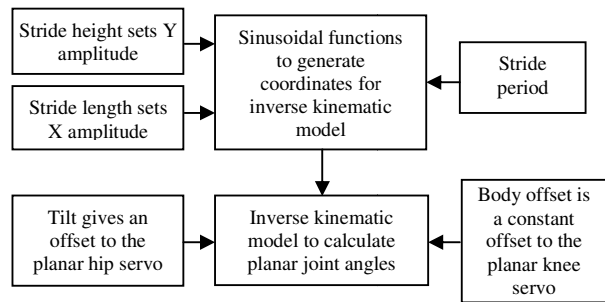


Fig. 8 Overview of robot kinematics of the hip, knee and foot servos with parallel axis.

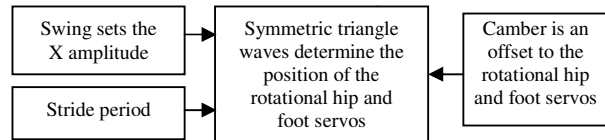


Fig. 9 Overview of lateral motion calculations.

### III. MEASUREMENT

A custom firmware in a lookup table form was developed that contains the inverse kinematics for the Bioloid Legs and all of the functions detailed above. A windows front end (Fig. 10) passes variables to the controller through a wireless ZigBee serial connection. The front end allows the user to dynamically alter all of the parameters of the model and quickly implement new parameter values in addition to allowing you to drive the robot remotely.

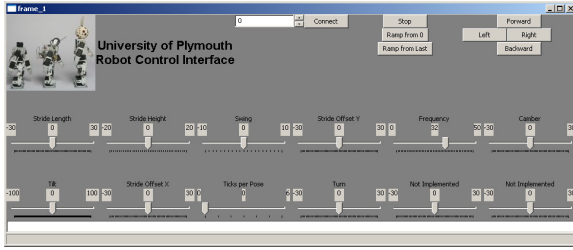


Fig. 10 PC based interface allows rapid adjustment of Gait Parameters.

### A. Gait quality measurements

The goal is to find a dynamic gait that produces the fastest possible travel while maintaining robustness in the face of perturbing external forces. The overall travel speed could be characterized by the product of the stride length and the stride frequency. Unfortunately, the feet slip by various amounts depending on the frictional coefficients between the robot's foot and the walking surface.

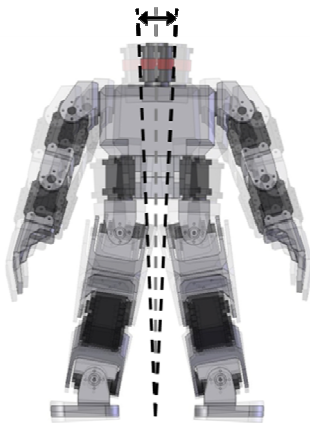


Fig. 11 Head displacement was measured as indicated.

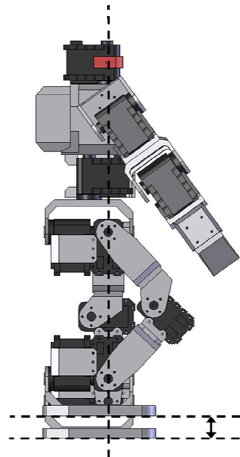


Fig. 12 Foot clearance quality was based on the foot completely leaving the surface.

Latt et al. [5] argue that human gait is optimised to maximize head stability. For the purpose of this study, head displacement perpendicular to the displacement of the robot (lateral displacement) was measured. The sagittal head motion was small relative to the lateral motion. Foot clearance was measured as a necessary condition for robot locomotion<sup>1</sup>. It should be noted that the maximum stride length is a function of actual foot clearance achieved given a set of gait parameters. If the feet do not clear the ground then the walk is inefficient or uncontrollable.

Head stability and foot clearance were measured as a function of stride period, stride height and swing. The various static parameters were not observed to have a significant effect on the desired measurements and the stride length was not observed to have a significant effect on the head stability as measured in the perpendicular plane.

In total sixty four data points were acquired corresponding to four data points for each the three variables. All the data were taken on a consistent surface of an extremely low nap carpet-like material. The feet of the robot were cleaned during the measurements and the temperature of the motors was monitored to insure the reproducibility of the measurements.

The head stability was measured using a pair of digital callipers by visually observing the displacements of the head between the callipers (Fig. 11). The uncertainty in these measurements was quite large as a result of the crude technique and measurements of the same system at different times led to an average percent uncertainty of 6%. The foot clearance was measured subjectively with 0 being a fail, and 1 through 3 being successful clearances with increasing clearance (Fig. 12).

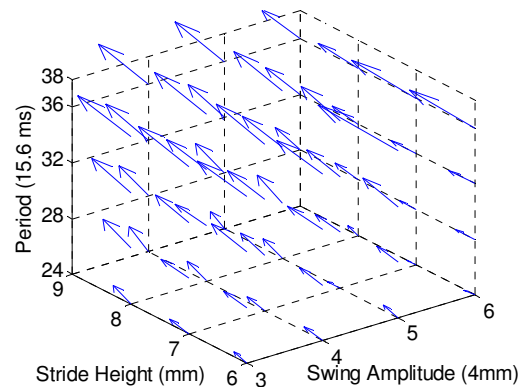


Fig. 13 3D parameters space and results. For each of the three variables four different values were tested resulting in  $4^3$  or 64 measurements. At each point in parameter space, a vector is drawn with the lateral head displacement as the horizontal component and the foot clearance as the vertical component. An ideal parameter set would result in a vector pointing vertically up.

<sup>1</sup> The actual foot clearance differs from the set stride height due to dynamic limitations of the servos and body posture dependences.

#### IV. DATA ANALYSIS

The results are plotted in three dimensions to show how the volume of the parameter space was investigated (Fig. 13). At each point in the parameter space, a vector is drawn with the lateral head displacement as the x coordinate and foot clearance as the y coordinate. An ideal parameter set should result in no lateral head displacement and a non-zero foot clearance. This would be represented by a vector pointing vertically up. Note: the head stability measured in mm is scaled to the same range as the foot clearance by dividing it by a scaling factor of five. No errors are indicated but it is important to remember that there is an average uncertainty in the length of each vector of 6%. Each of the variables will be examined as a 2D projection on the 3D graph (Fig. 13).

##### A. Period vs. Swing

Head stability shows a strong dependence on period and an additional dependence on swing amplitude. However, at the bottom most right of the graph (Fig. 14), the robot has become unstable at high values of stride height and fails to achieve the necessary foot clearance for lower values. The most promising region for further investigation is as indicated by the ellipse.

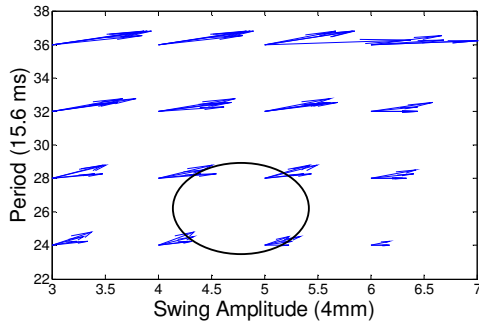


Fig. 14 Measured Quantities as a function of Period and Hip Swing amplitude. The multiple vectors at each point correspond to each of the measured stride heights.

##### B. Stride Height vs. Swing Amplitude

The robot has the greatest head stability in the lower right region of graph (Fig. 15) where the robot is not lifting its feet off the ground. These points are not useful for a dynamic walk since in order to walk, it must lift its feet. Moving toward the top portion of the graph, it is clear that both the head stability and the foot clearance are improved by moving to larger stride heights. The seemingly best values are grouped in the region indicated by the ellipse on the graph. This is a region calling for more detailed investigation.

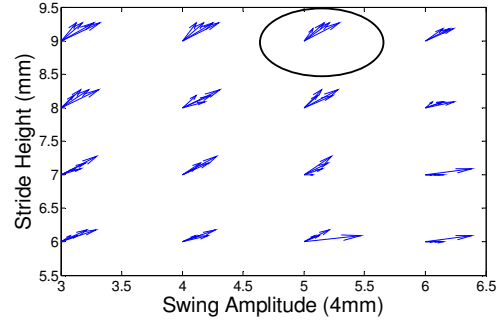


Fig. 15 Measured quantities as a function of stride height and swing amplitude. Each point contains four vectors corresponding to each of the periods.

##### C. Period vs. Stride Height

Here the positive effects of higher frequency on head stability are quite apparent. However, there is a countervailing effect that lower period leads to undesirably lower foot clearance. Only at large values of stride height does the robot reach acceptable values of foot clearance. The bottom right of this graph (Fig. 16) is the most promising region for further investigation.

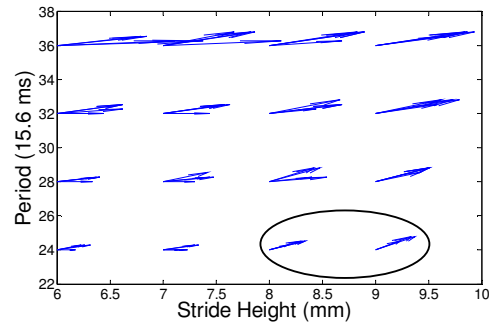


Fig. 16 Measured quantities as a function of period and swing amplitude. Each point contains four vectors corresponding to each of the stride heights.

Combining the analysis shown in Fig. 14, 15 and 16, we can indicate the bounds of the optimal head stability and foot clearance parameter space as an ellipsoid in Fig. 17.

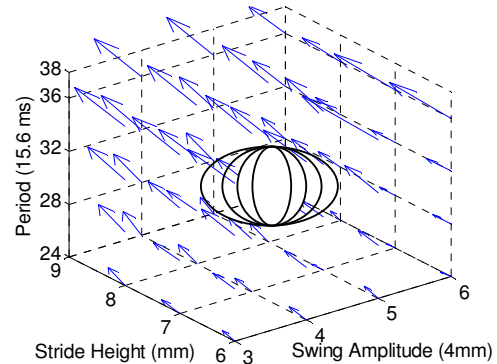


Fig. 17 Ellipsoid indicates the optimal region of parameter space for head stability and foot clearance.

## V. CONCLUSION AND FURTHER WORK

The parameters of stride height, swing and period that were identified as being important for head stability were each shown to have an effect on that stability as measured. The dependence of head stability on each of these variables was tested and a region of stable operation was identified. The tools that were developed were useful in evaluating gait parameters and show great promise in allowing further investigation as we change the geometry, servos and weight distribution of the robot.

We found that operating the robot with a shorter period, a median value for hip swing and maximizing the stride height led to increased head stabilization. Since two of these parameters were optimal at the limits of the parameter space explored in this study, the analysis should be extended to include additional regions. This study was further limited in that it used a fixed camber, body height and tilt. Adjusting these parameters may affect the optimal stability region for the overall robot. Preliminary measurements of the linear speed of the robot were made while operating in the current optimal volume of the parameter space and the robot was able to walk for 3 meters without falling at higher speeds than were previously achievable (up to  $0.22 \pm 0.011$  m/s compared with previous maximum speeds of  $0.14 \pm 0.008$  m/s).

In addition to further work mentioned above, the linear ramps used for the swing should be replaced with a function that more rapidly shifts the centre of mass over one foot and then leaves it there until the next foot is coming down. This would result in the centre of gravity being over the foot for a much longer time and thus reducing the amount of slippage that occurs as the biped walks. During the study, the arms were held fixed parallel to the sides of the biped. Arm oscillations can provide additional stabilization [6] and need to be investigated. Now that the region of stability has been identified, additional work is required to identify the most stable point within that region. In addition, while head stability is one measure of overall stability, it only addresses the stability of the robot in the axis perpendicular to the motion. The trajectories through the parameter space that allow for stable transitions between different locomotion speeds and rotations need to be investigated. With the tools developed, these additional investigations can be performed in a methodical way and should lead to increased optimisation of the biped's gait.

## ACKNOWLEDGEMENT

The authors would like to acknowledge the valuable contributions from Phil Hall and Joerg Wolf.

## REFERENCES

- [1] Mayer N, Ogino M, Guerra, R, Boedecker, J, Fuke S, Toyama H, Watanabe A, Masui K, Asada M "JEAP Team Description" RoboCup Symposium, 2008.
- [2] Behnke S, Online Trajectory Generation for Omnidirectional Biped Walking. In Proc. of 2006 IEEE International Conference on

- Robotics and Automation (ICRA'06), Orlando, Florida, pp. 1597-1603, May 2006.
- [3] Wolf J, Vicente A, Gibbons P, Gardiner N, Tilbury J, Bugmann G and Culverhouse P (2009) in Proc. FIRA RoboWorld Congress 2009, Incheon, Korea, August 16-20, 2009 (Springer Progress in Robotics: ISBN 978-3-642-03985-0) . pp. 25-33.
- [4] Wolf J, Hall P, Robinson P, Culverhouse P, "Bioloid based Humanoid Soccer Robot Design" in the Proc. of the Second Workshop on Humanoid Soccer Robots @ 2007 IEEE-RAS International Conference on Humanoid Robots, Pittsburgh (USA), November 29, 2007.
- [5] Latt M, Menz H, Fung V, Lord S. (2007) "Walking speed, cadence and step length are selected to optimise the stability of head and pelvis accelerations" *Experimental Brain Research* Vol 184: pp 201 – 209.
- [6] Shibukawa M, Sugitani K, Kasamatsu K, Suzuki S, Ninomija S (2001) "The Relationship Between Arm Movement and Walking Stability in Bipedal Walking" Accessed online Oct 1 2009. URL [handle.dtic.mil/100.2/ADA409793](http://handle.dtic.mil/100.2/ADA409793).